Materials Views
www.MaterialsViews.com

ADVANCED MATERIALS
www.advmat.de

COMMUNICATION

Upgraded Silicon Nanowires by Metal-Assisted Etching of Metallurgical Silicon: A New Route to Nanostructured Solar-Grade Silicon

Xiaopeng Li, Yanjun Xiao, Jin Ho Bang, Dominik Lausch, Sylke Meyer, Paul-Tiberiu Miclea, Jin-Young Jung, Stefan L. Schweizer, Jung-Ho Lee, and Ralf B. Wehrspohn**

Great efforts have been devoted in the last years to develop cost-effective silicon wafer technologies to cope with the dramatic price decrease for solar cell modules. A major restriction is still imposed by the high fabrication costs, especially at the step of purifying metallurgical grade silicon (MG-Si, purity ~99%) to solar grade (SG-Si, purity 99.9999%) or even electronic-grade (EG-Si, purity >99.999999%).[1,2] The challenge is to successfully develop solar grade silicon such as upgraded metallurgical silicon (UMG-Si) with reasonable cost and without sacrificing device efficiency and stability. On the other hand, silicon nanotechnology could offer an improved material efficiency to reduce the used amount of silicon and to reduce feedstock cost. However, current silicon nanotechnological approaches start from EG-Si[3–5] or use high temperature growth regimes for silicon nanowires (SiNWs) on mainly silicon substrates,[6,7] or a rather costly dry etching technique[8] to achieve reasonable device performance. Those approaches, though they are very interesting from a material perspective, do not address a cost-efficient way to produce nanotechnological silicon solar cells.

X.Li
Max-Planck Institute of Microstructure Physics
Weinberg 2, Halle 06120, Germany
X. Li, Dr. P.-T. Miclea, Dr. S. L. Schweizer, Prof. R. B. Wehrspohn
Institute of Physics
Martin-Luther-Universität Halle-Wittenberg, Halle 06099, Germany
Y. Xiao, J.-Y. Jung, Prof. J.-H. Lee
Department of Chemical Engineering
Hanyang University
Ansan, Kyounggi 426-791, South Korea
E-mail: jungho@hanyang.ac.kr
Prof. J. H. Bang
Department of Chemistry and Applied Chemistry
Hanyang University
Ansan, Gyeonggi-do 426-791, South Korea
D. Lausch, Dr. S. Meyer
Fraunhofer Center for Silicon Photovoltaics CSP
Halle 06120, Germany
Prof. R. B. Wehrspohn
Fraunhofer Institute for Mechanics of Materials IWM
Halle 06120, Germany
E-mail:Ralf. Wehrspohn@iwmh.fraunhofer.de

DOI:10. 1002/adma.201300973

We show in this contribution a way to tackle both challenges: Use dirty Si (MG-Si and UMG-Si) as a starting material and upgrade its purity to solar grade while nanostructuring it. The basic idea is based on the process of metal-assisted chemical etching (MaCE).[3,4] **Figure 1**a,b shows the schematic diagram for the SiNW synthesis by MaCE (for more details see methods section). In a nutshell, Si substrates are first loaded with dense Ag nanoparticles (AgNPs) by galvanic displacement, and subsequently etched in a HF and H_2O_2 solution. AgNPs drill nanoholes deep into the Si substrate. In the meantime, metal impurities such as their precipitates or silicides[9] are dissolved upon exposure to the acidic etchant solution. Consequently, SiNWs are purified as a result of the impurity removal.

Four different grades of silicon were used in the present study to verify the upgrading effect. These include MG-Si pieces and powder (**Figure 2**a,b; purity ~99.74%, from Q-Cells GmbH), UMG-Si (Figure 2c,d; multicrystalline, p-type, 0.2–0.5 Ω cm, purity ~99.999772%, from Fraunhofer IWM), SG-Si (see Supporting Information (SI), Figure S1, multicrystalline, p-type, 1–3 Ω cm, purity ~99.9999%, from Fraunhofer IWM) and EG-Si (Figure S2, monocrystalline, (100) orientation, 1–10 Ω.cm, purity >99.999999%, from Si-Mater GmbH).

Figure 2c,d shows scanning electron microscopy (SEM) images of SiNWs formed on a dirty UMG-Si wafer. Compared with MaCE of the polished EG-Si wafer (see Figure S2), the reaction of dirty UMG-Si is more complex. At first, much more hydrogen bubbles were generated than during the etching of EG-Si indicating a high silicon dissolution speed. Within a few minutes, morphological defects developed by wafer sawing were removed leaving behind NWs of good crystallinity as shown in Figure 2f. For the UMG-Si with different crystallographic grains, SiNWs in different grains were slanted in different angles but the etching directions generally followed the <100> direction. To confirm the reduced impurity level inside the UMG-Si after etching, we used inductively coupled plasma mass spectrometry (ICP-MS) element analyses, which are capable of tracing multi elements, at the part per trillion level. The impurity level of a ~50% etched wafer (see Figure S3) was compared with that of non-etched wafer as shown in **Figure 3**b. After MaCE, transitional metals all met reduced levels: Cr (92.6% reduction), Fe (74.3%), Ni (77.6%), Co (78.8%), Mo (79.6%), Cu (17.7%), and Ag (90.6%). The dopant levels such as B, P, and As were not changed, validating the high accuracy of our measurements. UMG-Si was thus upgraded from 99.999772 to 99.999899% in purity.

 © 2013 WILEY-VCH Verlag GmbH & Co. KGaA, Weinheim

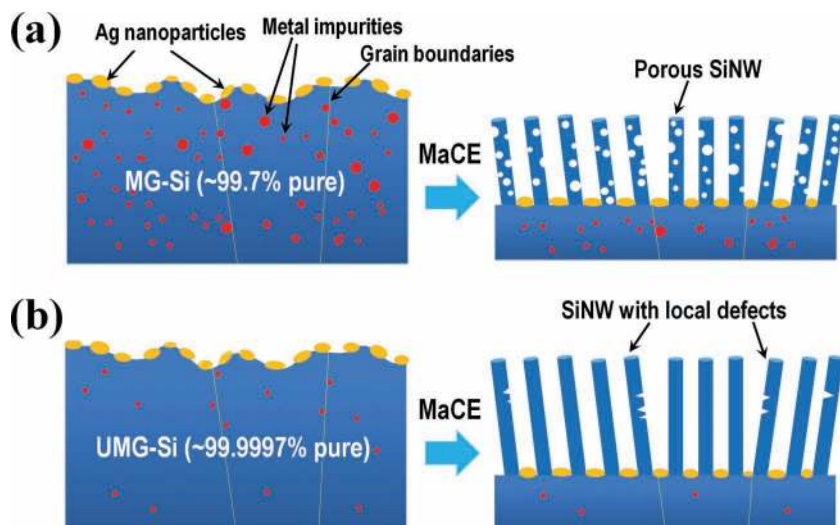

Figure 1. Schematic representation of the fabrication process of purified SiNWs from dirty silicon via metal assisted chemical etching (MaCE): (a) MG-Si, (b) UMG-Si.

To verify the advantages of upgraded UMG-SiNWs, we further investigated their optical and photo-electrochemical properties. More than 95% light absorption in the wavelength range of 300–1000 nm has been recorded from our optimized MaCE samples (see **Figure S6**), which is almost identical to the values reported from high-purity SiNWs prepared via MaCE of EG-Si[14] or other techniques such as chemical vapor deposition (CVD).[15]

The improved opto-electronic properties of the upgraded SiNWs were demonstrated by photo-electrochemical measurements as a proof of concept (**Figure 4**a,b). Indeed, *in-situ* measurements showed that with increasing etching time of the UMG-Si, the dark current was reduced (see Figure 4c). We speculated that this phenomenon was due to the successive removal of metal impurities, thus the

To verify this upgrading effect during MaCE of dirty silicon, we also etched MG-Si pieces (Figure 2a,b) and powder (see Figure S4). Similar to the UMG-Si a significant purity increase of the MG-Si powder was observed from 99.74 to 99.9881% after MaCE and the subsequent HNO_3 treatment further improved the purity to 99.9884% (Figure 3a). In contrast, $HF+H_2O_2/HNO_3$ acid washed (etching without Ag deposition) MG-Si can only purify the MG-Si powder to 99.975% (see SI, Table S1). Due to the high amount of impurities compared to UMG-Si, SiNWs etched from MG-Si pieces had not only etching pits on their surfaces but became entirely porous (see Figure 2a,b). The Super-X EDX (from FEI) spectrum of the MG-SiNWs (detection limit ~0.1%) shows no metal impurities in MG-SiNW, and the EDX mapping of different metal impurities only exhibited the background signals (see Figure S5), again confirming the MG-SiNWs were purified.

We believe that for the understanding of the upgrading effect by MaCE different aspects need to be considered: (I) The spatially inhomogeneous distribution of metal impurities inside multicrystalline dirty Si,[10–13] in particular at grain boundaries; (II) the redox-potential of the different metal species; (III) the effect of having dissolved metal ions into the etching solution and the interaction between them. More detailed analyses of the different effects of MaCE and the HNO_3 treatment are currently ongoing.

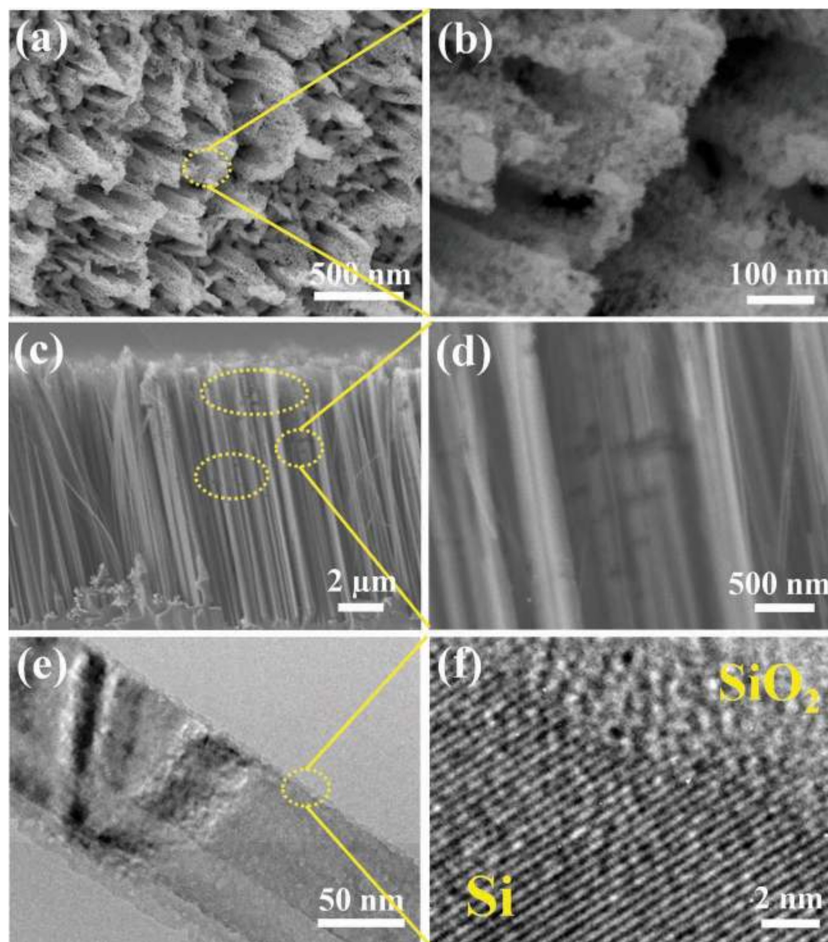

Figure 2. (a, b) SEM tilted-views of SiNWs etched from MG-Si. (c, d) SEM cross-sectional views of SiNWs etched from UMG-Si. (e, f) HRTEM images of UMG-SiNWs sonicated from the substrate at different maginification. The two dark bands in (e) are the local etching defects at NW surface.

© 2013 WILEY-VCH Verlag GmbH & Co. KGaA, Weinheim

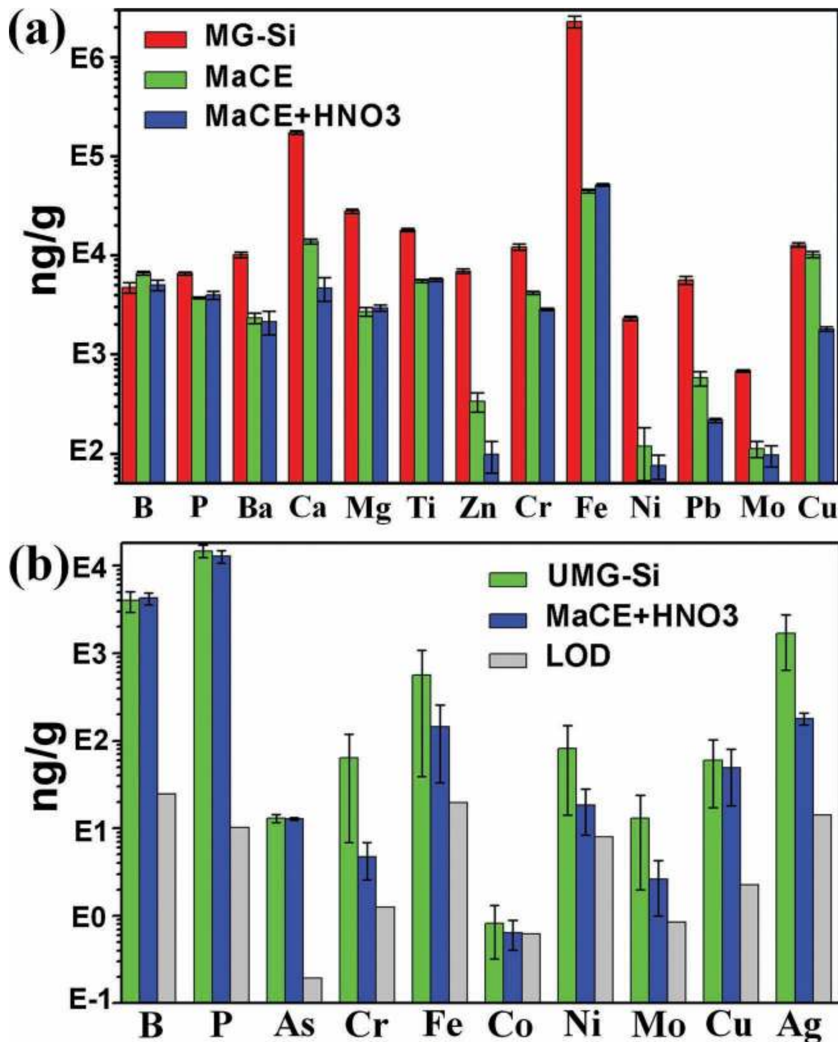

Figure 3. (a-b) The impurity level in raw MG-Si powders (red), MaCE processed (green) and MaCE+HNO_3 processed (blue) MG-Si powders. (b) The impurity level in clean (blue) and MaCE+HNO_3 processed (green) UMG-Si samples, in which the grey bars stand for the limit of detection (LOD). The error bars represent the standard deviations between multiple determinations.

material quality was improved. In contrast, such a decrease in dark current was not observed for the EG-SiNWs (see Figure 4c and Figure S7); moreover, the increase of metal impurities in EG-Si would greatly enhance the dark current (see Figure S8). On the next step, we measured the photocurrent-voltage (J-V) behavior of the UMG-SiNWs and EG-SiNWs, and their corresponding mother substrates (Figure 4d). The saturated photocurrent density of the EG-SiNWs was almost identical to its planar counterpart (J~6 mA/cm^2). In contrast, the photocurrent density of the UMG-SiNWs showed a 35% increase in photocurrent in comparison to the UMG-Si wafer verifying the upgrading effect.

Interestingly, the onset potential V_{os}, which is defined as the voltage where the photocurrent exceeds the dark current,[16] showed an anodic shift of 200 mV in the UMG-SiNWs in comparison to the polished UMG-Si wafer (Figure 4(d)). For the EG-SiNWs, this shift was greater than 400 mV. Similar to V_{oc} (open circuit potential) in a photovoltaic device, V_{os} is determined by the difference of the Fermi level in the dark and the electron quasi-Fermi level under illumination for bulk and NW configuration. It has been reported that due to 'electron pulling' by the terminating hydrogen, electrons would transfer from the Si core to the surface and change the band bending at the surface.[17] This charge transfer is negligible for bulk silicon but is significant for surface-dominated SiNW whose carrier concentration could be considerably higher. Hydrogen-terminated SiNWs would exhibit the increased hole concentration. Moreover, as shown in the HRTEM image in Figure 2f, the NW surface was rough, inducing many surface defects. Even with only a partial coverage of water absorbates on these defects, the hole concentration inside the NW can also be enhanced[17] by lowering the defect energy. As a result, the increased p-type doping of SiNW would decrease the space charge region (SCR) width, consequently lowering the Fermi level and leading to the anodic shift in V_{os}. Since the doping concentration of EG-Si was originally lower than that of the UMG-Si, the anodic shift in EG-Si was more pronounced after the NW creation. To further verify our assumption, we conducted impedance spectroscopy measurements, which can give critical quantitative information of the capacitance and the charge transfer resistance of the SCR and surface states.[18] If the NWs can effectively separate photogenerated carriers, the value of C_{SCR} for the NW sample should be higher than that for the planar sample due to increased junction area and hole concentration. This was indeed observed: the C_{SCR} of UMG-SiNWs etched for 5 min was 3 times higher than that of polished UMG-Si (see Figure S9). The charge transfer resistance R_{SCR} was reduced about 45 times, indicating easier charge separation. Figure 4e compares the stability of photocurrent during cycling of MaCE purified UMG-SiNWs and planar UMG-Si. The UMG-SiNWs exhibited a better stability than their mother substrate (planar UMG-Si), which proved that during water splitting NW structures likely tolerated oxidation more than the planar structure did.

In conclusion, we have investigated the MaCE characteristics of MG-Si and UMG-Si for the first time. Superior purification of dirty Si was observed, from 99.74 to 99.9884% for the MG-Si powder, and from 99.999772 to 99.999899% for the UMG-Si wafer during fabricating large areas of SiNWs on their dirty mother substrates. By photo-electrochemical tests, we verified that upgraded dirty SiNWs exhibited a superior performance over their mother substrates if the surface recombination was well controlled. Our approaches open a new way for upgrading MG-Si to solar grade, and have a great

© 2013 WILEY-VCH Verlag GmbH & Co. KGaA, Weinheim

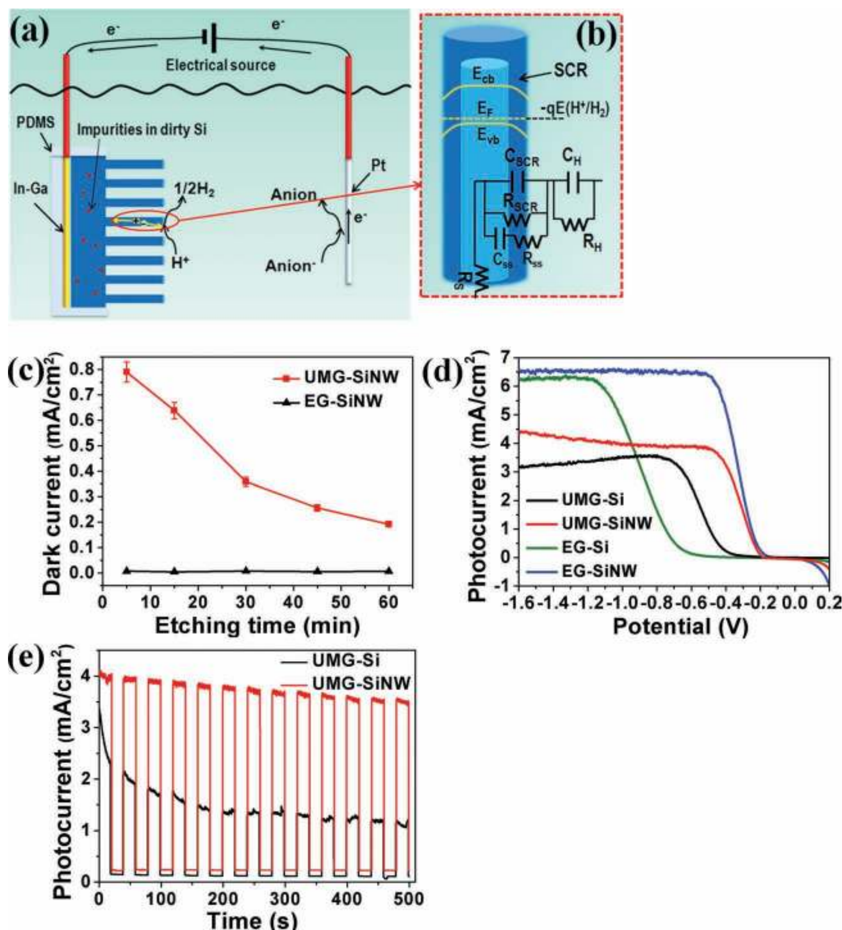

Figure 4. (a) Schematic of a PEC cell using p-type UMG-SiNW as a photocathode for hydrogen evolution. (b) Band bending and space charge region (SCR) formation of UMG-SiNW after immersing into the electrolyte. The equivalent circuit is also plotted. Rs is the series resistance. C_H and R_H is the capacitance and resistance of the Helmholtz layer. The same applies to the SCR, surface states (SS). (c) Dark current density versus etching time curve of UMG-SiNW (Red square) and EG-SiNW (black triangular). (d) Photocurrent densities (J) versus potential (V) curves under simulated solar illumination of EG-Si wafer (Cyan), EG-SiNW (5 mins etching) (Blue), polished UMG-Si (Black), and UMG-SiNW (5 mins etching) (Red). (e) Photocurrent responses of the UMG-Si (Black) and UMG-SiNW (Red) versus ON-OFF cycles of illumination at the potential –0.6 V.

potential to reduce the solar device cost without sacrificing the conversion efficiency.

Experimental Section

MaCE of different grades of Si: Silicon substrates were pre-cleaned in 5 wt% HF to remove native oxides. AgNPs were firstly deposited on silicon surfaces by immersing into the solution of 10 mM $AgNO_3$ + 5 M HF. Afterwards, silicon substrates were immersed into the solution containing 5 M HF and 0.3 M H_2O_2 to obtain SiNWs. For MG-Si powder etching, 25% ethanol was added to wet the particle surface. After each step of MaCE, the MG-Si powder needed to be filtered and washed using filter papers.

Photoelectrochemical measurements: For the photo-electrode fabrication, an ohmic contact was formed by smearing In-Ga eutectic on the backside of Si sample. Then, the sample was attached to a conductive copper tape. In order to protect the backside electrode from the acidic electrolyte, PDMS was used to encapsulate the backside of the sample.

The photoelectrochemical measurements were conducted using a CHI660D potentiostat (*CH Instruments, Inc.*) in a three electrode configuration. A saturated calomel electrode acted as the reference electrode and platinum mesh was used as counter electrode. The electrolyte was 0.5 M H_2SO_4. Prior to the photo-electrochemical measurements, the native oxide on the Si photo-electrodes was removed by a 3-minute-dip in a 5% HF solution. The light source used was a 150 W Solar Simulator from Newport Company. The light was guided by a single-branch fiber bundle from Oriel to the photo-electrode. The photo-electrochemical J-V curves were ramped from –1.6 V to 0.2 V (vs. Calomel electrode) at a rate of 50 mV/s.

Supporting Information

Supporting Information is available from the Wiley Online Library or from the author.

Acknowledgements

X. Li is grateful for the financial support from International Max-Planck Research School (IMPRS). The authors wish to thank Dr. Kai Petter from Q-Cells, Ramon Ordas, José Manuel Míguez Novoa from Grupo Ferroatlántica for providing metallurgical silicon. This work was supported in part by the National Research Foundation of Korea (NRF) grant funded by the Korea government (MEST) (No. 2011-0028604) and the BMBF-Research College StrukturSolar.

Received: April 3, 2013
Published online: May 2, 2013

[1] N. Yuge, M. Abe, K. Hanazawa, H. Baba, N. Nakamura, Y. Kato, Y. Sakaguchi, S. Hiwasa, F. Aratani, *Prog. Photovolt. Res. Appl.* **2001**, *9*, 203.
[2] P. Woditsch, W. Koch, *Sol. Ener. Mater. Sol. Cells* **2002**, *72*, 11.
[3] K.-Q. Peng, Y. Wu, H. Fang, X. Zhong, Y. Xu, J. Zhu, *Angew. Chem. Int. Ed.* **2005**, *44*, 2737.
[4] Z. Huang, N. Geyer, P. Werner, J. d. Boor, U. Gösele, *Adv. Mater.* **2011**, *23*, 285.
[5] X. Li, P. W. Bohn, *Appl. Phys. Lett.* **2000**, *77*, 2572.
[6] V. Schmidt, J. V. Wittemann, U. Gösele, *Chem. Rev.* **2010**, *110*, 361.
[7] H.-D. Um, S.-W. Jee, K.-T. Park, J.-Y. Jung, Z. Guo, J.-H. Lee, *J. Nanosci. Nanotech.* **2011**, *11*, 6118.
[8] J. Y. Kwon, D. H. Lee, M. Chitambar, S. Maldonado, A. Tuteja, A. Boukai, *Nano Lett.* **2012**, *12*, 5143.
[9] M. Seibt, K. Graff, *J. Appl. Phys.* **1988**, *63*, 4444.
[10] J. Dietl, *Solar Cells* **1983**, *10*, 145.

© 2013 WILEY-VCH Verlag GmbH & Co. KGaA, Weinheim

[11] X. Ma, J. Zhang, T. Wang, T. Li, *Rare Metals* **2009**, *28*, 221.
[12] S. A. McHugo, A. C. Thompson, I. Perichaud, S. Martinuzzi, *Appl. Phys. Lett.* **1998**, *72*, 3482.
[13] D. Laush, K. Petter, R. Bakowskie, J. Bauer, O. Breinstein, C. Hagendorf. *27th EUPVSEC*, DOI: 10.4229/27thEUPVSEC2012-2CO.13.4
[14] J.-Y. Jung, K. Zhou, H.-D. Um, Z. Guo, S.-W. Jee, K.-T. Park, J.-H. Lee, *Opt. Lett.* **2011**, *36*, 2677.
[15] T. Stelzner, M. Pietsch, G. Andrä, F. Falk, E. Ose, S. Christiansen, *Nanotechnology* **2008**, *19*, 295203.
[16] J. Oh, T. G. Deutsch, H.-C. Yuan, H. M. Branz, *Energy Environ. Sci.* **2011**, *4*, 1690.
[17] C.-S. Guo, L.-B. Luo, G.-D. Yuan, X.-B. Yang, R.-Q. Zhang, W.-J. Zhang, S.-T. Lee, *Angew. Chem. Int. Ed.* **2009**, *121*, 10080.
[18] G. Yuan, K. Aruda, S. Zhou, A. Levine, J. Xie, D. Wang, *Angew. Chem. Int. Ed.* **2011**, *20*, 2334.

© 2013 WILEY-VCH Verlag GmbH & Co. KGaA, Weinheim